PERGAMON

International Journal of Heat and Mass Transfer 42 (1999) 1237–1254

International Journal of HEAT and MASS TRANSFER

Modified effective thermal conductivity due to heat dispersion in fibrous porous media

Kuang-Ting Hsiao, Suresh G. Advani*

Department of Mechanical Engineering, University of Delaware, Newark, DE 19716, U.S.A.

Received 30 December 1997; in final form 20 July 1998

Abstract

When a fluid flows past an array of cylinders that represent the porous media, the micro convection around the cylinders will contribute to heat dispersion. The modified effective thermal conductivity tensor that includes the microscopic heat dispersion effect is usually calculated by a volume averaging method. This method requires a closure constitutive vector **b** to simulate the modified effective thermal conductivity tensor. In this paper, a direct temperature solution method to calculate the modified effective thermal conductivity tensor, by solving the temperature field in a unit cell with appropriate boundary conditions, is proposed. This method introduces a moving frame that converts the convective-diffusion equation in a pure conduction equation. Navier–Stokes equations and energy equations are solved in an array of cells and effective thermal conductivity is calculated from the local temperature field. The dependence of the modified effective thermal conductivity tensor on pertinent dimensionless numbers such as Peclet number, thermal conductivity ratio of solid to liquid, and the ratio of solid volume (volume fraction of the cylinders) in the unit cell is discussed.

Nomenclature

b closure vector function
c_p specific heat capacity
D total thermal diffusivity tensor
$\mathbf{D}^d$ hydrodynamic dispersion tensor
e unit vector in a Cartesian coordinate
h half height of a unit cell
I identity tensor
k thermal conductivity
$\mathbf{k}_e$ effective conductivity tensor for molecular diffusivity
$\mathbf{K}_d$ effective conductivity tensor for dispersion effect
K modified effective thermal conductivity tensor
K_{xx} modified effective thermal conductivity along the flow direction
K_{yy} modified effective thermal conductivity perpendicular to the flow direction
l length of a unit cell
n normal vector
P pressure
Pe Peclet number
q heat flux
Re Reynolds number
S surface
S_{fs} interface of fluid and solid phase
t time
T temperature
u velocity vector
$\mathbf{u_D}$ Darcy's velocity
$\mathbf{u}_{pcf}$ the reference velocity of the pure conduction frame
$\langle \mathbf{u} \rangle$ local volume averaged velocity vector
u x component of velocity
v y component of velocity
V local representative elementary volume
x coordinate vector
x, y, z Cartesian coordinates.

Greek symbols

α thermal diffusivity
ΔT imposed temperature difference
ε volume fraction
θ transformation of temperature
η viscosity

*Corresponding author. Tel.: 001 302 831 8975; fax: 001 302 831 3619; e-mail: advani@me.udel.edu

0017–9310/98/$ - see front matter
PII: S0017–9310(98)00246–4

Ψ the quantity to be applied in volume averaging theorem
ρ density.

Subscripts
f fluid phase
s solid phase
l moving reference frame or pure conduction frame.

Superscripts
$\hat{}$ deviation
– average
* dimensionless.

Others
$\langle\rangle$ local representative volume averaging operator
$\langle\rangle^{f}$ local representative fluid-phase volume averaging operator
$\langle\rangle^{s}$ local representative solid-phase volume averaging operator.

1. Introduction

In the composite manufacturing process, the heat transfer is an important issue. Especially for liquid injection molding process, such as resin transfer molding (RTM) and structural reaction injection molding (SRIM), a cold viscous resin flows through the preform of reinforcing fibers placed in a closed hot mold. The stationary fiber bed constitutes the fibrous porous media. The thermal convection due to the fluid motion and the thermal conduction between the fibers, resin and the interface effect the temperature of the resin in the fibrous porous media. The microscopic heat dispersion is expected to effect the macroscopic temperature history [1]. It is important to predict the temperature history accurately to prevent the resin from turning into a gel before the cavity is filled or from curing too fast and degrading the composite. For this, one needs a model that will account for the physics of heat transfer phenomena undergoing inside the mold that contains a network of fibers.

Volume averaging method [2] is used to describe the macroscopic energy equation through a porous media of stationary fiber bed. Darcy's velocity, $\mathbf{u_D}$, is used to describe the macroscopic fluid convection. However in porous media, the macroscopic convective term, $\mathbf{u_D}\cdot\nabla\langle T\rangle$, described by Darcy velocity is not sufficient to describe the hydrodynamic effect on heat transfer because of the hydrodynamic dispersion phenomena that prevail in porous media due to the non-uniformity of the local velocity in the pores of the fiber bed as shown in Fig. 1. Hence if we use the Darcy's velocity to describe the macroscopic convective term, we must account for the local heat dispersion in some way. One way is to include this effect into macroscopic conductive term [3]. Practice has converged on use of a modified effective thermal conductive term in the macroscopic energy equation to describe this behavior in a 'lumped' sense [4].

To explore and to predict the modified effective thermal conductivity tensor that accounts for heat dispersion in a two-dimensional porous media, we first employ the volume averaging method [2] and the concept of a unit cell model to represent the periodic structure of fiber performs. In this method, a vector function $\mathbf{b}$, which projects the gradient of averaged volume temperature onto the scalar function of local temperature deviation, is used to show the existence of the modified effective thermal conductivity tensor. Sahraoui and Kaviany [5] conducted two-dimensional numerical simulations of the total thermal diffusivity tensor by using $\mathbf{b}$ vector based on an order of magnitude analysis. The total thermal diffusivity tensor was given as $\mathbf{D} = \mathbf{k}_e/(\rho c_p)_f + \varepsilon_f \mathbf{D}^d$, where $\mathbf{k}_e$ is the effective conductivity tensor contributed by molecular diffusivity, and $\mathbf{D}^d$ is the hydrodynamic dispersion tensor of the fluid. However, the visualization of temperature field of the unit cell is still of interest since it will provide a clear physical understanding of the heat dispersion phenomenon.

Based on the understanding of the modified effective thermal conductivity tensor and the microscopic energy equation for non-isothermal flow of resin in stationary fiber bed, we have developed a direct temperature solution method to calculate the modified effective thermal conductivity tensor by applying the first law of thermodynamics to the unit cell. Our method is verified for the well known Taylor's solution [6]. Taylor's dispersion theory not only provides us with an analytical solution but also provides clues on how to solve for the microscopic semi-periodic temperature field inside the unit cell by selecting a moving observation frame which is traveling at the mean velocity of a flow through the porous media. With selected observation frame and boundary conditions, we solve for the semi-periodic temperature field in the unit cell. Then, the modified effective conductivity tensor for a fibrous porous media is calculated by using the direct temperature solution method and from the semi-periodic temperature field. Our results agree with the experiment data [7] and show the same trend provided by [8].

We used the software package, FIDAP7.05, to find the numerical solution. FIDAP solves the Navier–Stokes equations and energy equation for a fluid, based on the finite element method. This software package allows us to implement the user-defined subroutines and to simulate flow in any complex geometry and arrangement of a fiber preform. We focused on flow across a cylindrical fiber in a square unit cell, i.e., in-line cylindrical unit cell. Results obtained by using FIDAP were checked by comparing numerically calculated values of modified effective conductivity with the simple analytical solutions where available. We investigate the influence of relevant important dimensionless parameters such as Peclet num-

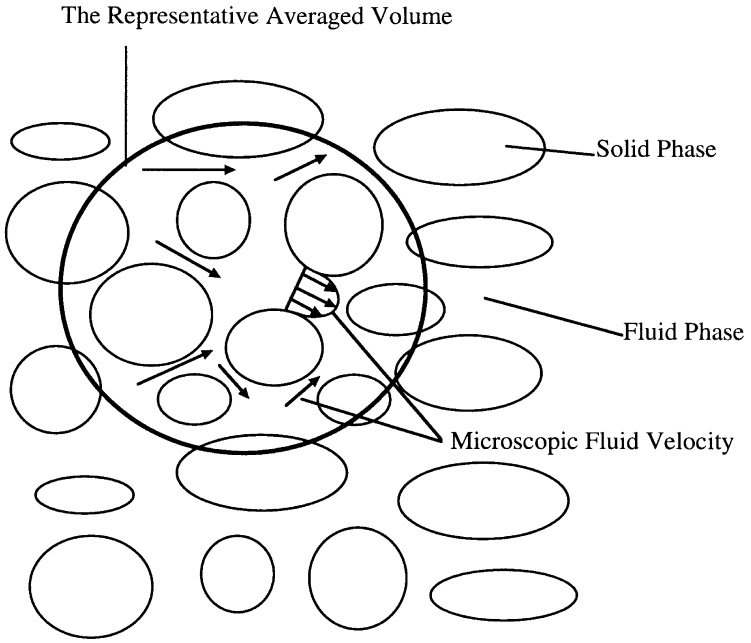

Fig. 1. The representative averaged volume and the non uniform microscopic velocity of a porous medium.

ber (Pe), porosity, and fiber-resin conductivity ratio on modified effective conductivity.

2. Previous work

In this paper, we will study the heat transfer of fluid across an aligned fiber bed at the unit cell level. Hence, here we shall review some important contributions that address the issue of heat dispersion in porous media.

Taylor [6] studied the dispersion in a tube, making appropriate assumptions based on experimental observations, he found an analytic solution for the axial dispersion coefficient which he non-dimensionalized with respect to the fluid molecular diffusivity, i.e., D^{d}_{xx}/α_f, and showed that it was related to Pe_f^2. Aris [9] further extended Taylor's dispersion coefficient to a total axial diffusion coefficient, D_{xx}/α_f, that combined the molecular diffusion and hydrodynamic dispersion effect. Scheidegger [10] used a stochastic model, the random walk model, to obtain the dependence of the axial dispersion coefficient on Pe_f^2 for ordered porous media and Pe_f for disordered porous media. De Josselin De Jong [11] employed similar analysis as Scheidegger's to get the heat dispersion effect in disordered porous media. In addition to the dependence of the axial dispersion coefficient on Pe_f, he found Pe_f dependence of the lateral dispersion coefficient D^{d}_{yy}/α_f. Saffman [12] modeled the micro structure of a disordered porous media as a network of capillary tubes randomly oriented at high Peclet numbers and under steady state conditions. He found that axial dispersion coefficient was proportional to $Pe_f \ln Pe_f$, and the lateral dispersion coefficient rose as Pe_f increased. Horn [13] developed a general method of moments based on Aris's [9] formulation, and solved for the axial dispersion coefficient as a function of Pe_f, porosity, and heat capacity ratio of fluid phase to solid phase. Brenner [14] obtained the dispersion tensor from the moments of the probability density of a particle position by extending Brownian theory for the particle in a periodic unit cell. Carbonell and Whitaker [2] used the local volume averaging technique to derive the macroscopic energy equation for a unit cell of porous media. In their approach, a vector function **b** was introduced, which projects the gradient of averaged volume temperature onto the scalar function of local temperature deviation. Eidsath et al. [15] employed the same technique to compute the total diffusion coefficient for the in-line cylinder unit cell with thermal conductivity of solid phase $k_s = 0$. Their results showed $Pe_f^{1.7}$ dependence for the axial total diffusion coefficient, D_{xx}/α_f, and the lateral total diffusive coefficient, D_{yy}/α_f, was almost constant. Koch et al. [16] derived a closure-form of expression for the dispersion tensor for a packed bed of spherical particles. They assumed equal thermal conductivities and heat capacities for the fluid and solid phase. Their results show the axial total diffusion coefficient was proportional to Pe_f^2, and the lateral total diffusion coefficient remained almost constant. Mei [17] applied the method of homogenization in a periodic unit cell and deduced the dispersion tensor in

terms of the microscale flow inside the unit cell. Yuan et al. [18] employed a thick wall tube model to study heat dispersion in porous media. Their results show the total axial diffusion coefficient D_{xx}^{d}/α_f, is proportional to Pe_f^2. As the thermal conductivity ratio of solid phase to fluid phase, i.e., k_s/k_f, increases, the D_{xx}/α_f increases at low Peclet number and decreases at high Peclet number. The heat capacity ratio of solid phase to fluid phase, $(\rho c_p)_s/(\rho c_p)_f$, also influences the axial total diffusion coefficient in their study. Zhang and Advani [3] employed the local volume averaging technique derived by Carbonell and Whitaker [2] to compute the **b**, and then calculated the axial dispersion coefficients on an in-line cylinder unit cell. Their results predict that D_{xx}^{d}/α_f is proportional to Pe_f^2. Sahraoui and Kaviany [5] used the same local volume averaging technique to compute the total diffusion coefficients of an in-line cylindrical unit cell. Their result agreed with Yuan et al.'s results [18] for the dependence of both Peclet number and conductivity ratio. They further showed that the lateral total diffusion coefficient, D_{yy}/α_f, remains almost constant for in-line cylinder arrangement and increases with Peclet number for staggered cylinder unit cell arrangement.

3. Volume averaged energy equation and modified effective thermal conductivity tensor

In porous media, velocity is not only non uniform in magnitude, but also changes direction at the pore level (Fig. 1). The porosity, geometry and arrangement of fibers could be extremely complex. Hence a practical solution is to consider the volume averaged energy equation for general porous media developed by Carbonell and Whitaker [2].

Consider the porous media in a representative volume V with stationary solid phase V_s and flowing fluid phase V_f as shown in Fig. 1.

The energy equations on a microscopic scale in the fluid phase and in the solid phase are

$$\frac{\partial T_f}{\partial t}+\nabla\cdot\mathbf{u}_f T_f=\nabla\cdot\alpha_f\nabla T_f \quad \text{in } V_f, \tag{1}$$

$$\frac{\partial T_s}{\partial t}=\nabla\cdot\alpha_s\nabla T_s \quad \text{in } V_s. \tag{2}$$

Note that the energy equation for solid phase is observed in a stationary frame and hence the convection term is zero. The local thermal equilibrium assumption is $\langle T_f\rangle^f=\langle T_s\rangle^s=\langle T\rangle$, where the $\langle\rangle$ denotes the average value over the unit cell. Assuming

$$T=\langle T\rangle+\hat{T}=\langle T\rangle+\mathbf{b}(\mathbf{x})\cdot\nabla\langle T\rangle \tag{3}$$

$$\mathbf{u}_f=\langle\mathbf{u}_f\rangle^f+\hat{\mathbf{u}}_f. \tag{4}$$

Note the fluid phase average velocity $\langle\mathbf{u}_f\rangle^f=\langle\mathbf{u}_f\rangle/\varepsilon_f=\langle\mathbf{u}\rangle/\varepsilon_f=\mathbf{u}_D/\varepsilon_f$, where $\mathbf{u}_D$ is Darcy's velocity. Here $\mathbf{b}(\mathbf{x})$ is a vector function that relates the gradient of the averaged volume temperature to the temperature deviation. The volume averaging theorem is

$$\langle\nabla\Psi_f\rangle=\nabla\langle\Psi_f\rangle+\frac{1}{V}\int_{S_{fs}}\Psi_f\mathbf{n}_{fs}\,dS. \tag{5}$$

Combining the local thermal equilibrium assumption and eqns (1)–(5), we obtain the volume averaged energy equation [4]

$$\{\varepsilon_f(\rho C_p)_f+\varepsilon_s(\rho C_p)_s\}\frac{\partial\langle T\rangle}{\partial t}+(\rho C_p)_f\langle\mathbf{u}_f\rangle\cdot\nabla\langle T\rangle=\nabla\cdot\{(\mathbf{k}_e+\mathbf{K}_d)\cdot\nabla\langle T\rangle\} \tag{6}$$

where we define the effective conductivity tensor for molecular diffusivity as

$$\mathbf{k}_e=(\varepsilon_f k_f-\varepsilon_s k_s)\mathbf{I}+\frac{k_f-k_s}{V}\int_{S_{fs}}\mathbf{n}\mathbf{b}\,dS. \tag{7}$$

The effective conductivity tensor for dispersion effect is defined as

$$\mathbf{K}_d=-\frac{(\rho C_p)_f}{V}\int_{V_f}\hat{\mathbf{u}}_f\mathbf{b}\,dV=-\frac{\varepsilon_f(\rho C_p)_f}{V_f}\int_{V_f}\hat{\mathbf{u}}_f\mathbf{b}\,dV. \tag{8}$$

For convenience, we further define a modified effective thermal conductivity tensor $\mathbf{K}=\mathbf{k}_e+\mathbf{K}_d$, which includes the molecular diffusivity and dispersion effects. The modified effective thermal conductivity tensor is independent of $\langle T\rangle$ and $\nabla\langle T\rangle$ and is expected to be a function of structure, volume fraction, conductivity ratio of solid to fluid phase, Reynolds number of the fluid, and the Peclet number of the fluid. One way to understand these effects is by using the **b** method [2, 8].

In this paper, alternatively, we will solve the modified effective thermal conductivity tensor by direct temperature solution based on energy balance in the control volume of a selected moving observation frame which is derived from the local thermal equilibrium model in an arbitrary observation frame. The generalized local thermal equilibrium model will include the convection of both the fluid phase and solid phase in an arbitrary observation frame. A characteristic velocity of the moving observation frame to eliminate the macroscopic heat convection term of the macroscopic energy equation is computed. The characteristic velocity is found to be useful for solving the microscopic temperature field directly. The results from direct temperature solution do agree with the results obtained by using the **b** method and local thermal equilibrium assumption. The visualization of microscopic temperature field in a unit cell is possible by this technique.

4. Direct temperature solution

Let us ignore the viscous dissipation and re-write the heat flux through a unit cell by using volume averaging

method in an arbitrary frame instead of a stationary frame.

$$\langle \mathbf{q}_{\text{total}} \rangle = \langle \mathbf{q}_{\text{convective}} \rangle + \langle \mathbf{q}_{\text{conductive}} \rangle$$
$$= \frac{1}{V}\left\{ \int_{V_f} \rho_f c_{p_f} \mathbf{u}_f T \, dV + \int_{V_s} \rho_s c_{p_s} \mathbf{u}_s T \, dV \right\} + \frac{1}{V}\left\{ -k_f \int_{V_f} \nabla T \, dV - k_s \int_{V_s} \nabla T \, dV \right\}. \quad (9)$$

Now we assume local thermal equilibrium and substitute $\mathbf{u}_f = \langle \mathbf{u}_f \rangle^f + \hat{\mathbf{u}}_f$, $\mathbf{u}_s = \langle \mathbf{u}_s \rangle^s$, and $T = \langle T \rangle + \mathbf{b} \cdot \nabla T$ into eqn (9). By using the volume averaging theorem, we can show the calculation of $\mathbf{b}$ vector can be replaced by the calculation of modified effective thermal conductivity that carries a physical meaning and can be readily used in macroscopic heat transfer equation to describe the thermal physical phenomena in a porous media;

$$\langle \mathbf{q}_{\text{total}} \rangle = \{ \rho_f c_{p_f} \langle \mathbf{u}_f \rangle + \rho_s c_{p_s} \langle \mathbf{u}_s \rangle \} \langle T \rangle - \mathbf{K} \cdot \nabla \langle T \rangle. \quad (10)$$

Eqn (6) is a particular case of eqn (10) when the observation frame and the solid phase are stationary, i.e., $\mathbf{u}_s = 0$. However, one should note that both eqn (6) and eqn (10) are based on the local thermal equilibrium assumption and the approximation of the microscopic temperature with the leading terms of Taylor's series. The equivalent heat flux of eqns (6) and (10) can be asserted only if those assumptions are realized in the unit cell.

When the solid is a transversely isotropic medium, the modified effective thermal conductivity tensor in two dimensions can also be written as $\mathbf{K} = K_{xx}\mathbf{e}_x\mathbf{e}_x + K_{yy}\mathbf{e}_y\mathbf{e}_y$. Using the averaging theorem, we can show that

$$\langle \nabla T \rangle = \langle \nabla T_f + \nabla T_s \rangle = \nabla \{ \langle T_f \rangle + \langle T_s \rangle \} = \nabla \langle T_f + T_s \rangle = \nabla \langle T \rangle. \quad (11)$$

The smallest volume to which one may apply the averaged energy equation is the unit cell. After solving the temperature field inside a unit cell, one can use eqn (10) and eqn (11) to calculate the modified effective thermal conductivity tensor.

Another interesting feature of eqn (10) is that we can convert it to pure macroscopic conduction equation in a selected observation frame, (t_1, x_1, y_1, z_1), which makes $\rho_f c_{p_f} \varepsilon_f \langle \mathbf{u}_f \rangle^f + \rho_s c_{p_s} \varepsilon_s \langle \mathbf{u}_s \rangle^s = \mathbf{0}$. In this selected frame, the steady state energy balance will be described as

$$\langle \mathbf{q}_{\text{total}} \rangle = -\mathbf{K} \cdot \nabla_1 \langle T \rangle, \quad \text{in } (t_1, x_1, y_1, z_1) \quad (12)$$

and the steady state macroscopic energy equation should be governed by pure steady state conduction equation as

$$0 = \nabla_1 \cdot (\mathbf{K} \cdot \nabla_1 \langle T \rangle), \quad \text{in } (t_1, x_1, y_1, z_1) \quad (13)$$

which is much simpler to solve as compared to a convective-diffusive equation. We will select the frame of reference with a velocity such that we eliminate the convective term and solve only eqn (13). In most porous media flows, the solid phase is stationary, and if we define the x direction along the direction of Darcy's velocity, $\mathbf{u}_D = \langle \mathbf{u}_f \rangle = u_D \mathbf{e}_x$, then to solve the equation in the selected frame, (t_1, x_1, y_1, z_1), which should move with a constant velocity $\mathbf{u}_{\text{pcf}}$ as

$$\mathbf{u}_{\text{pcf}} = \frac{(\rho c_p)_f u_D}{(\rho c_p)_f \varepsilon_f + (\rho c_p)_s \varepsilon_s} \mathbf{e}_x = \frac{u_D}{\varepsilon_f + \varepsilon_s [(\rho c_p)_s / (\rho c_p)_f]} \mathbf{e}_x. \quad (14)$$

This frame from now on will be referred to as pure conduction frame or moving reference frame, (t_1, x_1, y_1, z_1). One can find out that the velocity of pure conduction frame is identically the same as the thermal pulse velocity found by Carbonell and Whitaker [2].

4.1. Verification

In this section we will verify our approach and results for the modified effective thermal conductivity by comparing them with reported analytic solutions. Here we employ the Taylor [6] dispersion theory of flow between two infinite parallel plates as shown in Fig. 2.

The 2D energy equation of the fluid for the fully developed flow is

$$\frac{\partial T}{\partial t} + \frac{3}{2}\bar{u}\left(1 - \frac{y^2}{h^2}\right)\frac{\partial T}{\partial x} = \alpha_f \left(\frac{\partial^2 T}{\partial x^2} + \frac{\partial^2 T}{\partial y^2} \right) \quad (15)$$

where $\bar{u}$ is the magnitude of the average fluid velocity. The initial and boundary conditions are

$$T(0, x \neq x_0, y) = T_i \quad \text{and} \quad T(0, x_0, y) = T_o$$
$$T(t, \infty, y) = T_i \quad \text{and} \quad \frac{\partial T}{\partial y}(t, x, 0) = \frac{\partial T}{\partial y}(t, x, \pm h) = 0. \quad (16)$$

Taylor described this problem in the observation frame moving with mean velocity, i.e., $x_1 = x - \bar{u}t$, $y_1 = y/\text{h}$, $t_1 = t$. He further assumed $\partial T/\partial t_1 \sim 0$ & $\partial T/\partial x_1 \sim$ const after the elapsed time and neglected the axial conduction (see Fig. 2(c)). Using the above assumption and with $\theta = T - T_i$, we can solve the temperature field and then calculate the averaged convective heat flux across the plates perpendicular to x_1 as

$$\frac{\langle q_{\text{convective}} \rangle}{(\rho c_p)_f} = -\frac{1}{210} Pe^2 \alpha_f \frac{\partial \bar{\theta}}{\partial x_1} = -D_{xx}^d \frac{\partial \bar{\theta}}{\partial x_1} \quad (17)$$

where Peclet number $Pe = Pr \cdot Re = \bar{u}(2h)/\alpha_f$ is the relative strength of convection to molecular diffusion, and $\bar{\theta}$ is the average of θ for the cross section perpendicular to x_1. We can non-dimensionalize the dispersion coefficient with respect to molecular diffusivity as $D_{xx}^d/\alpha_f = Pe^2/210$. The total effective diffusivity [9] can be written as

$$\frac{D_{xx}}{\alpha_f} = 1 + \frac{1}{210} Pe^2 = 1 + \frac{D_{xx}^d}{\alpha_f}. \quad (18)$$

To verify our approach to calculate the modified effective conductivity tensor, one can use eqn (14) to verify that $u_{\text{pcf}} = \bar{u}$. Then using eqns (10)–(12) and eqn (17), one gets

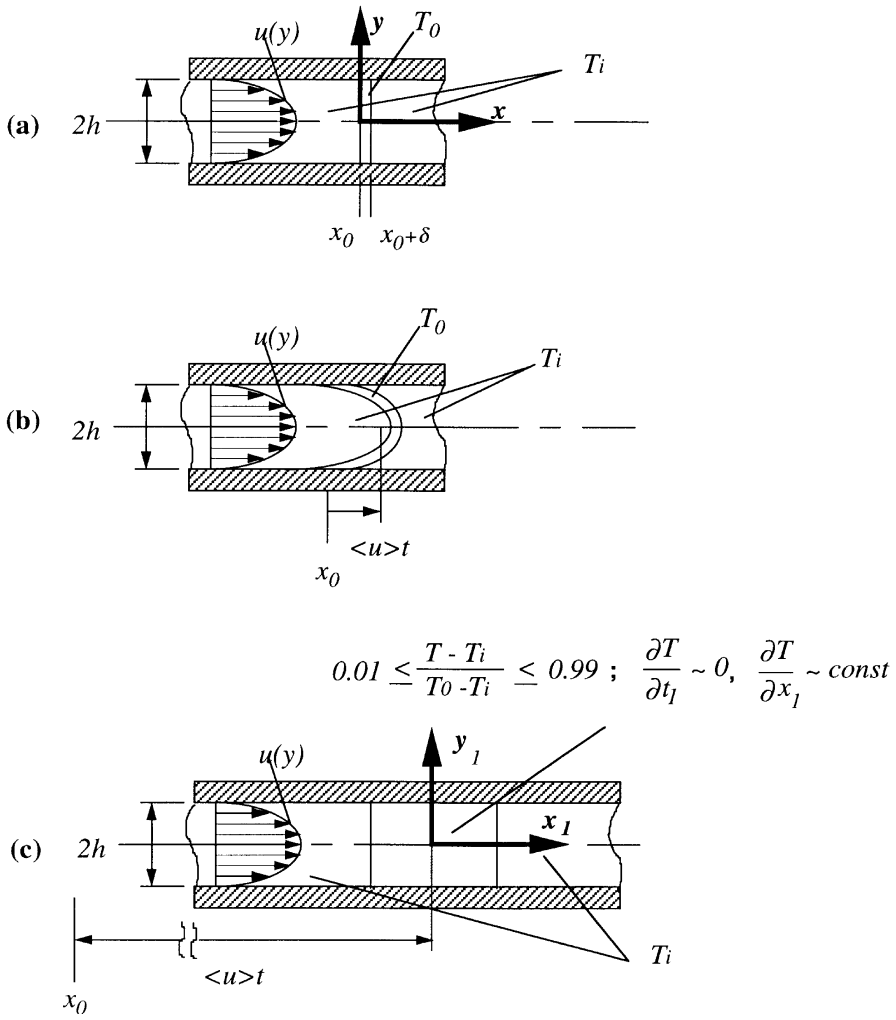

Fig. 2. Hydrodynamic dispersion in a fully developed flow between two parallel plates: (a) initial temperature field; (b) pure hydrodynamic dispersion; before the developed time; (c) molecular dispersion + pure hydrodynamic dispersion; after the elapsed time ($t \gg 1$).

$$K_{xx} = \frac{\langle q_{\text{total}} \rangle}{-\dfrac{\partial \theta}{\partial x_1}} = \frac{-\dfrac{1}{210} Pe^2 \rho c_p \alpha_f \dfrac{\partial \bar{\theta}}{\partial x_1} - k_f \dfrac{\partial \bar{\theta}}{\partial x_1}}{\dfrac{\partial \bar{\theta}}{\partial x_1}} = \left(\frac{1}{210} Pe^2 + 1 \right) k_f \quad (19)$$

and non-dimensionalizing the modified effective axial thermal conductivity based on the thermal conductivity of the fluid phase results in

$$K_{xx}^* = \frac{K_{xx}}{k_f} = 1 + \frac{1}{210} Pe^2 = 1 + \frac{D_{xx}^d}{\alpha_f} = \frac{D_{xx}}{\alpha_f}. \quad (20)$$

Equation (20) is identical to eqn (18). This will allow us to directly find the modified effective conductivity and circumvent the calculations of the **b** field.

Here, we notice that the observation frame selected by Taylor corresponds to our eqn (14). If we select an arbitrary plane perpendicular to x_1 as our unit cell, Taylor's quasi-steady state and constant temperature gradient assumptions, reduce to the pure macroscopic conduction phenomenon, described by eqn (12) and eqn (13). The microscopic temperature field of the unit cell and the particular solution of the macroscopic energy equation are consistent with the laws of energy balance.

We have derived and verified the direct temperature

solution method, which is based on fundamental mathematics and with clear physical meaning. The method can be used to find the modified effective thermal conductivity that reflects the dispersive effect if we have the periodic velocity and semi-periodic temperature field applied to the unit cell representing the porous media. Since the direct temperature solution method is based on the analysis of macroscopic energy equation and the physics of energy balance, it won't depend on the way we compute the **b** vector. The direct temperature solution method is similar to the experimental method which determines the modified effective thermal conductivity tensor from the physics and the given form of macroscopic energy equation. The macroscopic energy equation used in experimental analysis should be constructed on the basis of physical laws such as continuity, energy balance, and also frame independence. Most of the researchers construct the macroscopic energy equations in the stationary frame because of the simplicity, however, some generalized information such as use of the pure conduction frame can be lost. Use of a moving observation frame simplifies the analysis and allows one to determine effective thermal conductivity. We initiate the process by defining a unit cell along with appropriate boundary conditions to create the periodic velocity and semi-periodic temperature field inside the unit cells in the following section.

5. The direct temperature solution of periodic in line unit cells

We consider a periodic fiber arrangement, in which each fiber is a circular cylinder. The flow is perpendicular to the fiber and is two dimensional as the fiber length is usually much longer than its diameter. The schematic of the unit cell with in-line circular cylinder arrangement is shown in Fig. 3.

In this section, we will discuss the boundary conditions and unit cell geometry used to create the semi-periodic temperature field to solve for K_{xx} and K_{yy}. Based on eqn (10), eqn (14), and Taylor's dispersion theory, we know that it will be more efficient to solve for K_{xx} in a moving frame. It is also known that applying a constant temperature drop perpendicular to the direction of fully developed flow between two parallel plates will give us a fully developed temperature profile. We will exploit this to obtain a reasonable model to solve for K_{yy}, which we will discuss separately.

5.1. Modified effective thermal conductivity along the flow direction (K_{xx})

To solve for K_{xx}, we define two frames to observe the velocity and temperature field inside the unit cells, one is the stationary frame, (x, y, t), and the other is the pure conduction frame, (x_1, y_1, t_1), moving with constant velocity, $\mathbf{u}_{pcf} = u_{pcf}\mathbf{e}_x$, as described by eqn (14). The relation between the two frames is $x_1 = x - u_{pcf} \cdot t$, $y_1 = y$, $t_1 = t$. The governing equations for the stationary frame, (x, y, t) are

$$\left.\begin{aligned} &\mathbf{u}_s = \mathbf{0} \\ &\nabla \cdot \mathbf{u}_f = 0 \\ &\rho_f\left(\frac{\partial \mathbf{u}_f}{\partial t} + \mathbf{u}_f \cdot \nabla \mathbf{u}_f\right) = -\nabla P_f + \eta \nabla^2 \mathbf{u}_f \\ &\rho c_p\left(\frac{\partial T}{\partial t} + \mathbf{u} \cdot \nabla T\right) = k \nabla^2 T \end{aligned}\right\} \quad \text{in} \quad (x, y, t) \tag{21}$$

where the energy equation applies to both the fluid and the solid phase. And using the chain rule and material invariant principles, we can cast the governing equations for the moving frame, (x_1, y_1, t_1), similar to eqn (21) except $\mathbf{u}_s = -\mathbf{u}_{pcf}$.

Based on the understanding of Taylor's dispersion, we make the following assumptions,

$$\frac{\partial \mathbf{u}_f}{\partial t} = \mathbf{0}, \quad \text{in } (x, y, t)$$

$$\frac{\partial T}{\partial t_1} \sim 0, \quad \text{in } (x_1, y_1, t_1). \tag{22}$$

Note the quasi-steady state assumption of temperature in the moving frame is based on the asymptotic behavior of large elapsed time and dimensionless analysis. Using

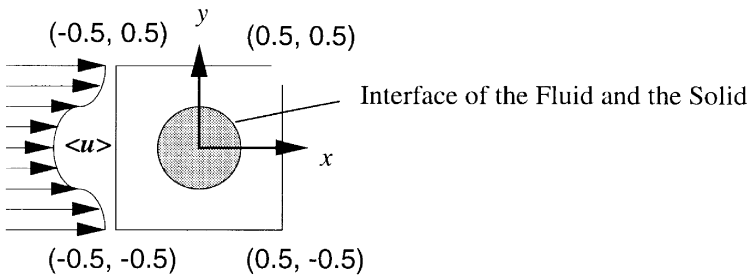

Fig. 3. In-line unit cell in a two-dimensional periodic architecture of a fibrous porous medium.

chain rule and eqn (22), we recast the motion equations in the pure conduction frame as

$$\rho_f\left(u_{pcf}\cdot\frac{\partial \mathbf{u}_f}{\partial x_1}+\mathbf{u}_f\cdot\nabla\mathbf{u}_f\right)=-\nabla P_f+\eta\nabla^2\mathbf{u}_f,$$

for the fluid phase in (x_1, y_1, t_1) (23)

$$\mathbf{u}_s=-u_{pcf}\cdot\mathbf{e}_{x_1},\quad \text{for the solid phase in } (x_1, y_1, t_1) \tag{24}$$

and the energy equations become

$$(\rho c_p)_f\cdot\mathbf{u}_f\cdot\nabla T_f=k_f\nabla^2 T_f,$$

for the fluid phase in (x_1, y_1, t_1) (25)

$$-(\rho c_p)_s u_{pcf}\mathbf{e}_{x_1}\cdot\nabla T_s=k_s\nabla^2 T_s,$$

for the solid phase in (x_1, y_1, t_1). (26)

At the interface of the solid and the fluid phase, we have the no-slip velocity boundary condition and equal heat flux boundary condition in the stationary frame (x, y, t) given by

$$\mathbf{u}_f=\mathbf{u}_s=\mathbf{0}$$

$$\mathbf{n}\cdot k_s\nabla T_s=\mathbf{n}\cdot k_f\nabla T_f, \text{ along the interface, in } (x, y, t) \tag{27}$$

and for pure conduction frame (x_1, y_1, t_1) these boundary conditions become

$$\mathbf{u}_f=\mathbf{u}_s=-u_{pcf}\mathbf{e}_{x_1}\mathbf{n}\cdot k_s\nabla T_s=\mathbf{n}\cdot k_f\nabla T_f,$$

along the interface, in (x_1, y_1, t_1) (28)

note the interface is moving in the pure conduction frame and has the same velocity as the solid phase in the pure conduction frame, i.e., relative velocity to the pure conduction frame.

Now we consider the other boundary conditions (BCs) for velocity. First, we will discuss the velocity field BCs in the stationary frame (x, y, t), since it had reached steady state in the stationary frame. Then we can transfer them to the pure conduction frame, (x_1, y_1, t_1), simply by eliminating the frame velocity $\mathbf{u}_{pcf}$.

The fully developed velocity profile can be created by the flow through a series of precursory unit cells as shown in Fig. 4, with the following boundary conditions,

$$\frac{\partial u}{\partial y}=0 \quad \text{and} \quad v=0,$$

at symmetry line or center line in (x, y, t) (29)

$$\frac{\partial u}{\partial x}=0 \quad \text{and} \quad v=0, \quad \text{at outflow in } (x, y, t). \tag{30}$$

We need to input an inflow velocity profile to keep the total flow rate equal to the product of Darcy's velocity multiplied by the height of the unit cell, i.e., $u_D\cdot 2h$. With respect to eqn (29), we assume

$$\frac{u_{guessed}(y)}{u_D}=\frac{-240}{7}\left(\frac{y}{h}\right)^4+\frac{120}{7}\left(\frac{y}{h}\right)^2 \quad \text{and} \quad v=0, \quad \text{at inflow in } (x, y, t) \tag{31}$$

where h is the height of the unit cell. We should note that this assumption is helpful in approaching the fully developed velocity profile at the outflow of the precursory unit cells by using fewer precursory unit cells. Other guesses for inflow profile may cost more precursory unit cells but should lead to the same result. Note one can transform the velocity boundary conditions from stationary frame (x, y, t) to the pure conduction frame (x_1, y_1, t_1) simply by subtracting the effect of $\mathbf{u}_{pcf}$.

For periodic structures such as our unit cell, we have the following description of semi-periodic temperature due to the volume averaged temperature gradient,

$$\frac{1}{2h}\int_{-h}^{h}[T(x_1+l, y_1)-T(x_1, y_1)]\,dy_1=\frac{\partial\langle T\rangle}{\partial x_1}\cdot l, \text{ in } (x_1, y_1, t_1) \tag{32}$$

where $2h$ is the height of the unit cell, and l is the length of the unit cell. Differentiating equation (32) and using eqn (13), we get

$$\int_{-h}^{h}\left[\frac{\partial T}{\partial x_1}(x_1+l, y_1)-\frac{\partial T}{\partial x_1}(x_1, y_1)\right]dy_1=0, \text{ in } (x_1, y_1, t_1). \tag{33}$$

Since the structure of the unit cell is periodic, we expect the temperature gradient of the unit cell to be the same at each periodic location and the temperature profile to be self similar. We assume the semi-periodic temperature conditions are given by

$$T(x_1+l, y_1)=T(x_1, y_1)+l\frac{\partial\langle T\rangle}{\partial x_1}$$

$$\frac{\partial T}{\partial x_1}(x_1+l, y_1)=\frac{\partial T}{\partial x_1}(x_1, y_1), \text{ in } (x_1, y_1, t_1) \tag{34}$$

where (x_1, y_1) can be any arbitrary position, and

$$\frac{\partial T}{\partial y_1}=0, \quad \text{at symmetry line or center line in } (x_1, y_1, t_1). \tag{35}$$

We complete our system as summarized in Figs 4 and 5. However, since this system is developed under a lot of assumptions, it is necessary to understand the capability of our system. To evaluate our system, we check the energy balance of the unit cell. When $(\rho c_p)_s/(\rho c_p)_f=1$, the energy of this unit cell balances exactly. And some accuracy loss is found when $(\rho c_p)_s/(\rho c_p)_f\neq 1$. The accuracy loss may come from those assumptions used to approach our system, for example, the local thermal equilibrium assumption, the quasi-steady state assumption, and the semi-periodic temperature boundary conditions. To improve the accuracy, more advanced and generalized theory may be needed in the future. Here, we will only use $(\rho c_p)_s/(\rho c_p)_f=1$ for our case study. Before solving

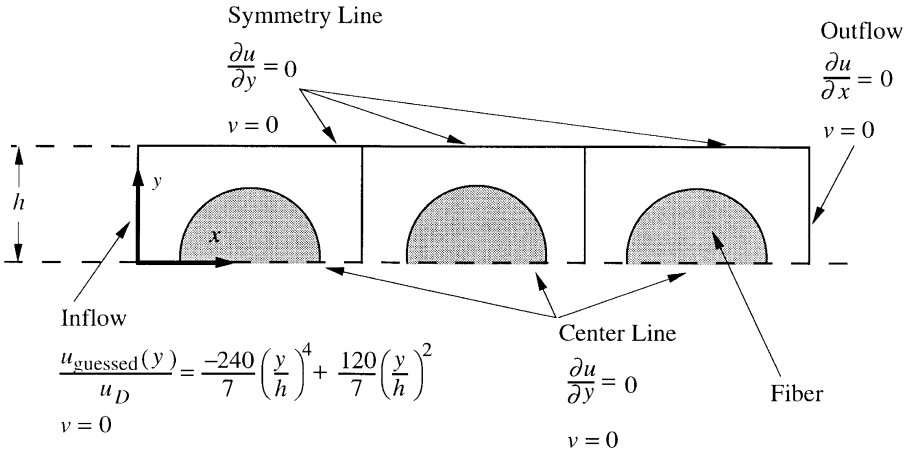

Fig. 4. Precursory unit cells and boundary conditions to create the fully developed velocity profile for the target unit cell (described in stationary frame).

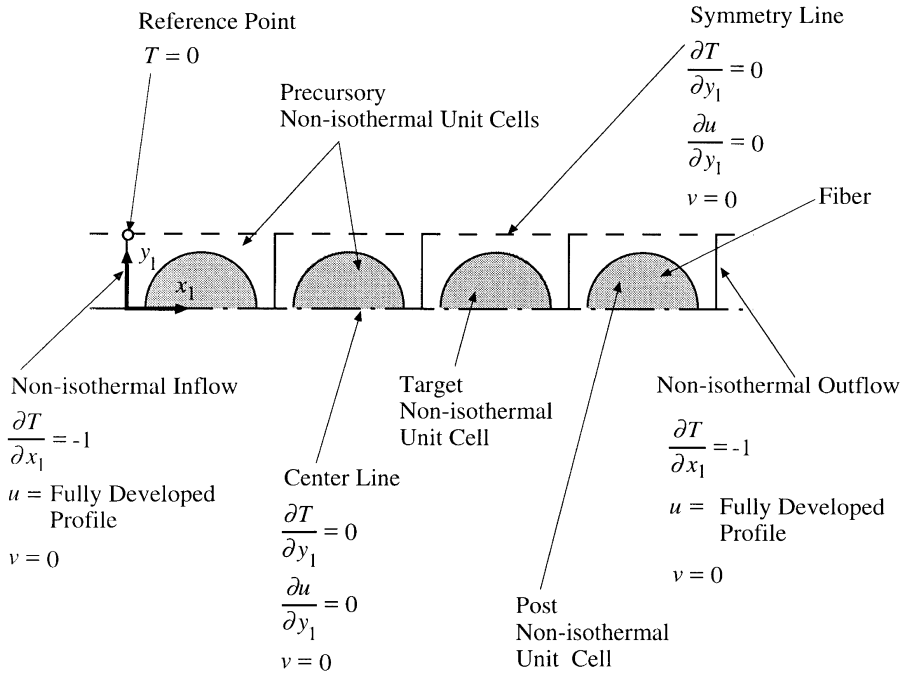

Fig. 5. Boundary conditions for a series of non-isothermal unit cells to solve for K_{xx} (described in the pure conduction frame).

the cell problem by FIDAP, we select our parameters as the ones for a typical resin transfer molding process, i.e., the conductivities of fluid and of solid are of the same order and setting $(\rho c_p)_s/(\rho c_p)_f = 1$. For numerical simulations, we apply uniform heat flux through the cross sections of inflow and outflow for a series of unit cells, and let the temperature profile develop through the unit cells. For our simulation, i.e., in-line unit cell, we use two precursory non-isothermal unit cells, one target non-isothermal unit cell, and one post non-isothermal unit cell. Figure 5 shows the unit cells with temperature boundary conditions. The numerical results show that

our approach with the semi-periodic temperature boundary conditions, i.e., the temperature profiles at the inlet and outlet of the target non-isothermal unit cell are similar to each other in the moving reference frame. Note here, instead of applying eqn (34) directly to the cell problem, we let the temperature profile develop through a series of unit cells naturally. The temperature profile solved by FIDAP will approach the semi-periodic temperature conditions, i.e., eqn (34).

For convenience, we further use the following dimensionless variables for the moving frame (x_1, y_1, t_1)

$$u^* = u/u_D, \quad v^* = v/u_D$$
$$x_1^* = x_1/l, \quad y_1^* = y_1/l$$
$$P^* = \frac{P}{\rho_f u_D^2}, \quad \eta^* = \frac{\eta}{\rho_f u_D^l} = \frac{1}{Re}$$
$$\rho_f^* = \rho_s^* = 1$$
$$k_f^* = 1, \quad k_s^* = \frac{k_s}{k_f}$$
$$c_{p_f}^* = \frac{u_D l}{\alpha_f} = Pe_f, \quad c_{p_s}^* = \frac{(\rho c_p)_s u_D l}{k_f} = Pe_f \cdot \frac{(\rho c_p)_s}{(\rho c_p)_f} = Pe_f. \tag{36}$$

Note that the solid is stationary, and without any contribution from inertial force. For convenience, we set $\rho_s^* = \rho_f^* = 1$. Hence, we expect $K_{xx}/k_f = K_{xx}^*$ (Re, Pe_f, ε_s, structure, k_s/k_f, $(\rho c_p)_s/(\rho c_p)_f$). One can use eqns (10)–(12) to calculate K_{xx} after solving the semi-periodic temperature field of the non-isothermal unit cell.

5.2. Modified effective thermal conductivity perpendicular to the flow direction (K_{yy})

To achieve the periodic temperature field to solve for K_{yy}, we can apply a constant temperature drop along the top and bottom symmetry lines of the unit cell in the stationary frame. The steady state governing equations and the interface BCs are eqns (21) and (27) respectively. The velocity BCs are eqns (29)–(31). To solve for K_{yy}, the periodic temperature boundary conditions of the inflow and outflow are

$$T(x+l, y) = T(x, y)$$
$$\frac{\partial T}{\partial x}(x+l, y) = \frac{\partial T}{\partial x}(x, y). \tag{37}$$

And at the symmetry line and the center line we have

$$T = \frac{\Delta T}{2}, \quad \text{along the top symmetry line} \tag{38}$$

$$T = 0, \quad \text{along the center line.} \tag{39}$$

The BCs for the non-isothermal target unit cell to solve for K_{yy} are summarized in Fig. 6. Here, we use the same

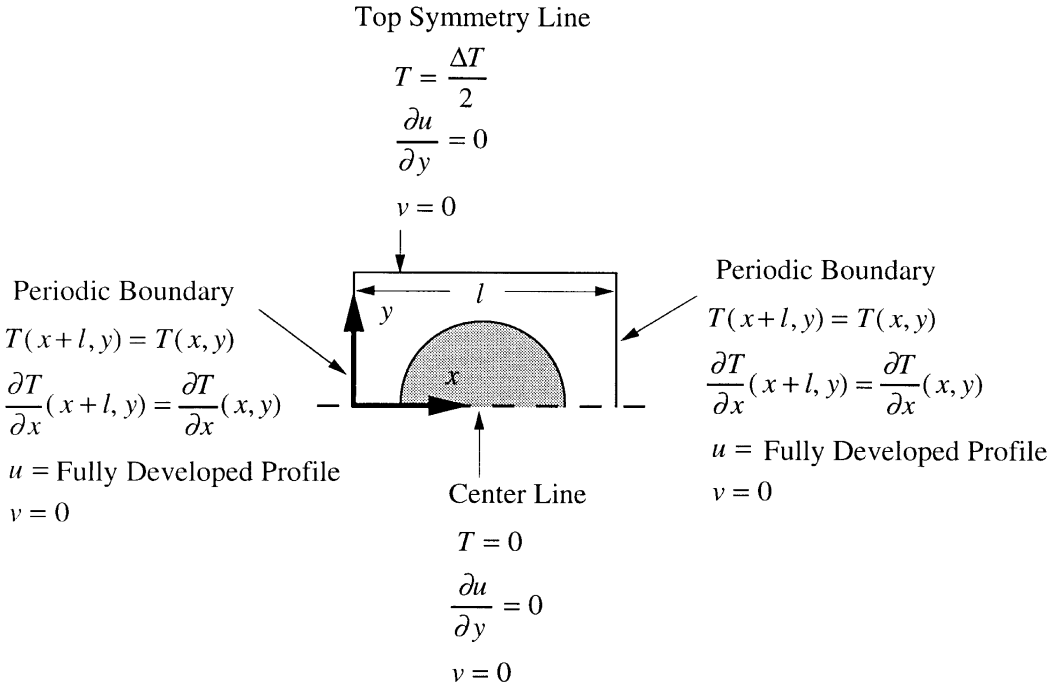

Fig. 6. Boundary conditions for the non-isothermal target unit cell to solve for K_{yy} (described in the stationary frame).

dimensionless variables as shown in eqn (36) and add $T^* = T/\Delta T$. Since $(\rho c_p)_s$ makes no contribution to this unit cell problem, we expect K_{yy}/k_f to be a function of K_{xx}^* (Re, Pe_f, ε_s, structure, k_s/k_f) from our analysis.

6. Numerical solution

We employed FIDAP7.05 to obtain the numerical solution of the flow field and the temperature distribution inside the unit cells with appropriate boundary conditions. FIDAP, Fluid Dynamics Analysis Package, is a general purpose computer program that uses the finite element method to solve the Navier–Stokes equations and the energy equation inside a given geometry. After the solution of the velocity field and the temperature field is obtained, FIPOST, i.e., post process module of FIDAP, is used to display streamlines, temperature contours etc. and also to calculate the heat flux values at the boundaries as well as the volume averaged temperature gradient of the target unit cell.

With FIDAP we solved the system of steady state, laminar, nonlinear Navier–Stokes equations and the energy equation. The extra term in the motion equation, eqn (23), observed in the pure conduction frame (x_1, y_1, t_1) was supplied by a subroutine as body force term in the Navier–Stokes equations. The motion equations were solved in the fluid region of the unit cell and the energy equation was solved for both the solid and the fluid. The velocity of solid phase is specified as the relative velocity to the observation frame. The no-slip boundary conditions were specified at the fluid and the solid interface. We provide an initial guess for the velocity profile, eqn (31), at the inflow boundary of the precursory unit cells to approach the fully developed flow (Fig. 4). The BCs shown in Figs 5 and 6 are applied on the non-isothermal unit cells to solve for the non-dimensional temperature field. The material properties used as input are in the non-dimensional system as shown in eqn (36).

After solving for the temperature profile inside the target unit cell, we use eqns (10)–(12) to calculate the modified effective thermal conductivity tensor in dimensionless form.

6.1. Verification

We compared the analytic solutions of the previous cases with the numerical solutions obtained from FIDAP. For Taylor's dispersion analysis, using 30×100 elements to mesh a thin plate (0.1×2) perpendicular to x_1 axis and for $Pe = 100$, we found that $K_{xx}^* = 47.61870$, with the error less than 2.05E-5.

7. Results and discussion

A parametric study was carried out to investigate the influence of various dimensionless parameters on effective thermal conductivity in the in-line unit cell. The inertial effect in RTM process is expected to be very weak as $Re < 1$, so we don't vary Reynolds number in this numerical study. We select $Re = 0.5$, $Pe_f = 0 \sim 600$, $\varepsilon_s = 0.1,\ 0.5$, $k_s/k_f = 0.1,\ 1,\ 10$, $(\rho c_p)_s/(\rho c_p)_f = 1$ as the parameters for most of the cases. These parameters are typical of the RTM process [4]. Some typical temperature distributions in a unit cell are shown in Fig. 7.

7.1. The dimensionless modified effective thermal conductivity along the flow direction (K_{xx}/k_f)

Since the convective heat transfer is strongly dependent on Pe_f, we expect K_{xx}/k_f to be dominated by heat conduction at $Pe_f = 0$, and by heat convection as Pe_f increases. Based on this qualitative understanding of heat dispersion inside the unit cell, we try to explain the influence of each parameter on K_{xx}/k_f.

- Peclet number of the fluid (Pe_f): As most reported studies in the literature, our results in Figs 8 and 9 show a strong dependence on Pe_f^2. Figure 8 shows that our numerical results agree with the experimental results done by Gunn and Pryce [7]. If we use power law to fit our results, the $Pe_f^{1.68} \sim Pe_f^{1.85}$ dependence at high Peclet number is obtained. Our power law trend study agrees well with the reported works [8, 15].
- Thermal conductivity ratio of the solid and the fluid (k_s/k_f): Fig. 10 depicts the effect of k_s/k_f on K_{xx}/k_f. At high Pe_f, the modified effective thermal conductivity K_{xx}/k_f increases as k_s/k_f decreases. The opposite trend is found at low Pe_f. However, the ratio of the modified effective thermal conductivities of two unit cells with different k_s/k_f approaches to a constant value as Pe_f approaches infinity. Similar results were reported by Sahraoui and Kaviany [5] and Yuan et al. [18].
- Volume fraction of solid (ε_s): The dependence of volume fraction should be related with other parameters, since it does not explicitly show up in the governing equations. The ε_s influences the geometry and the velocity of the reference moving frame (pure conduction frame) if $(\rho c_p)_s/(\rho c_p)_f \neq 1$. In this paper, we set $(\rho c_p)_s/(\rho c_p)_f = 1$, which deters us from relating the effect of ε_s and $(\rho c_p)_s/(\rho c_p)_f$ on K_{xx}/k_f. The local velocity deviation of the fluid and the surface of the interface of the solid increase as ε_s increases and provides a positive contribution to the heat convection. Our results show the K_{xx}/k_f increases as ε_s especially at high Pe_f. At low Pe_f, the contribution of ε_s is positive if $k_s/k_f \geqslant 1$.

7.2. The dimensionless modified effective thermal conductivity perpendicular to flow direction (K_{yy}/k_f)

In general, the molecular diffusivity is more important than the hydrodynamic dispersion for K_{yy}/k_f, but the

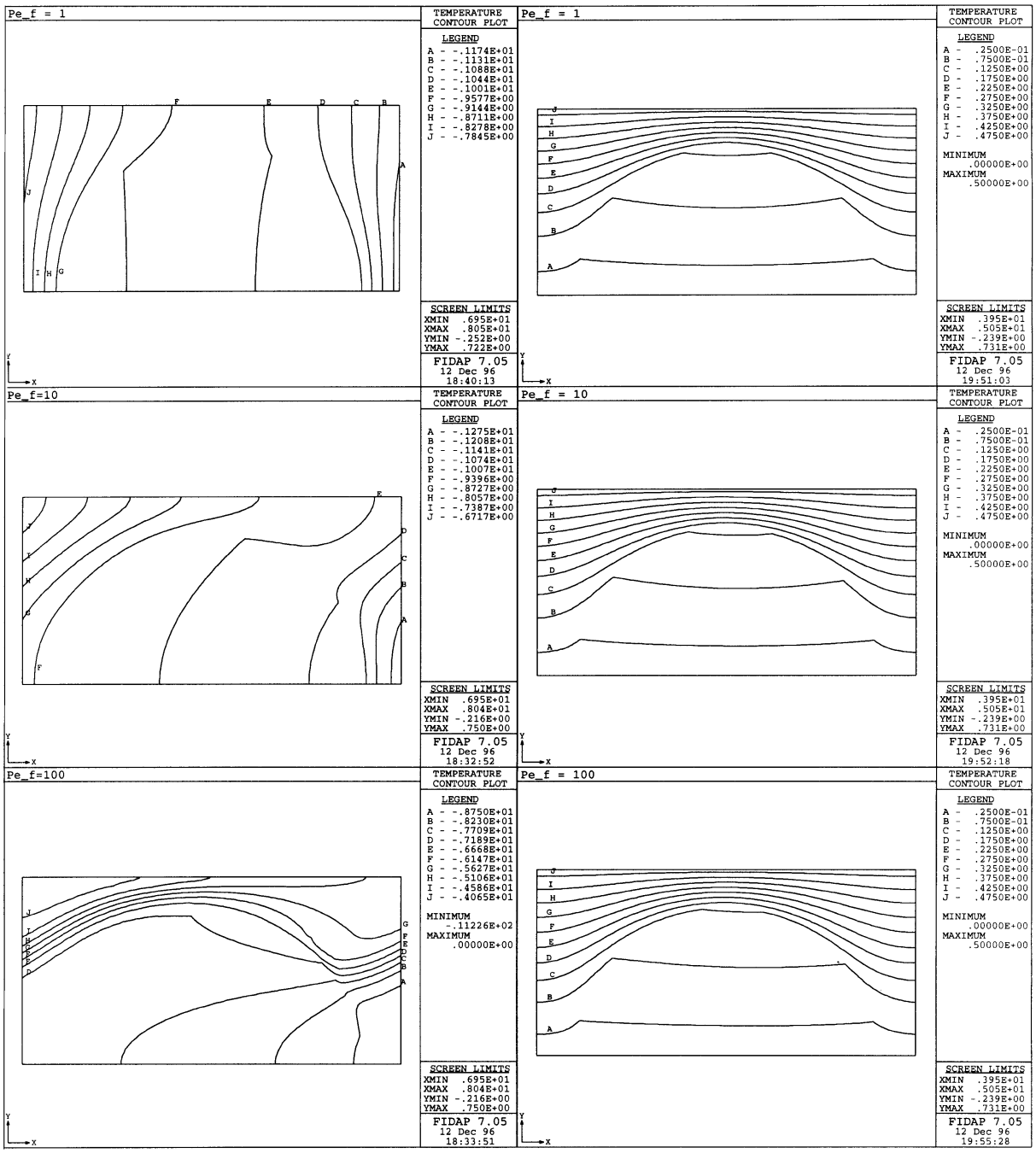

Fig. 7. The microscopic temperature contours in a unit cell: left side, the gradient of volume averaged temperature is in the flow direction; right side, the transverse gradient of volume averaged temperature. Note the in-line fibrous unit cell has the conductivity ratio of 10, the heat capacity ratio of 1, and the volume fraction of fibers of 50%.

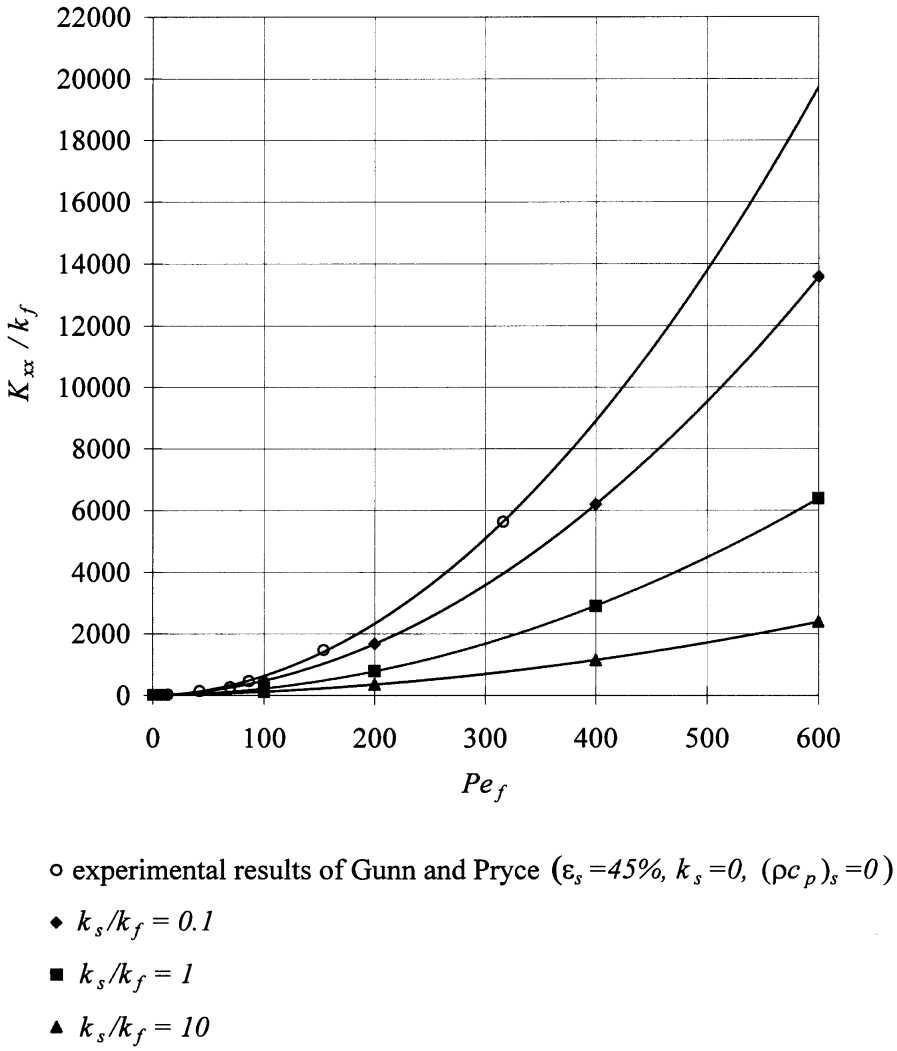

Fig. 8. The modified effective thermal conductivity along the flow direction vs Peclet number (solid volume fraction of 50%, heat capacity ratio of 1).

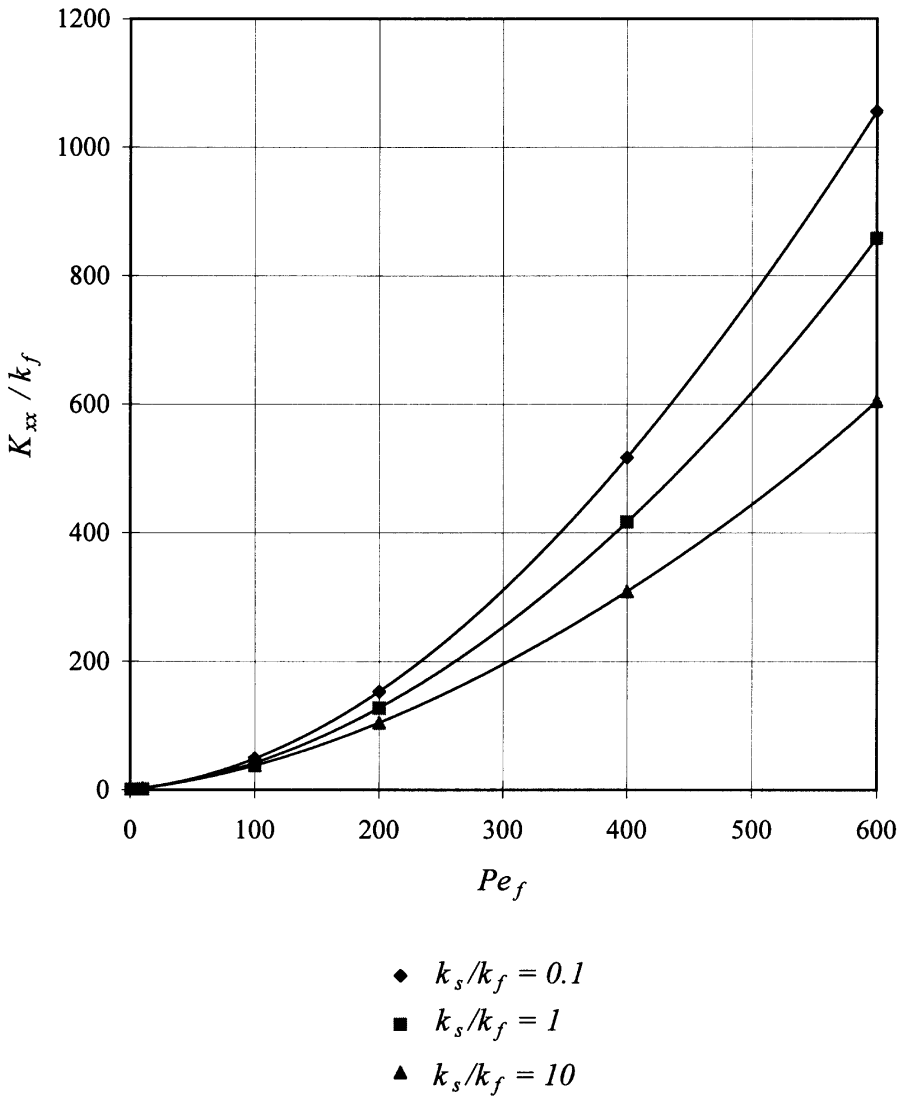

Fig. 9. The modified effective thermal conductivity along the flow direction vs Peclet number (solid volume fraction of 10%, heat capacity ratio of 1).

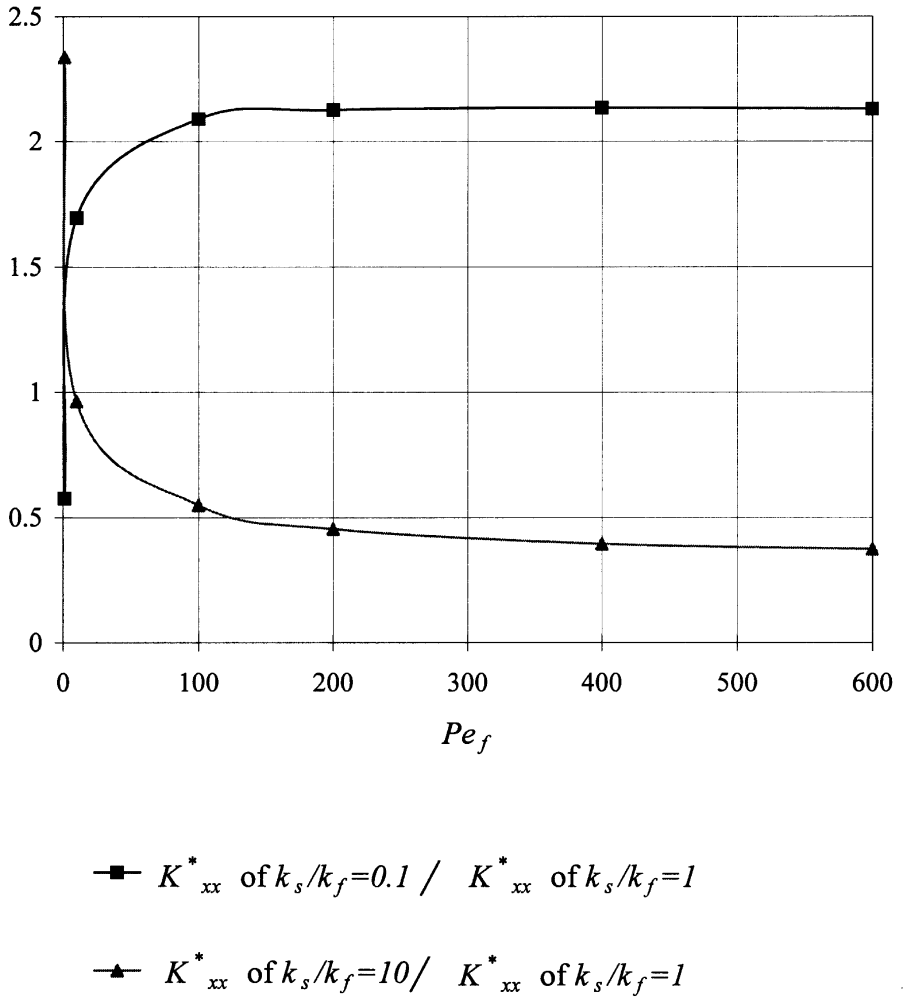

Fig. 10. The effect of k_s/k_f on K_{xx}/k_f (solid volume fraction of 50%, heat capacity ratio of 1).

error may be up to 20% if we neglect the hydrodynamic dispersion effect. These results are shown in Figs 11 and 12.

- When Peclet number increases, the effect of heat convection grows. But the increasing contribution by heat convection is small because only very small temperature gradient along the local flow direction is allowed to occur inside an in-line unit cell with imposed volume averaged temperature gradient perpendicular to the Darcy's flow direction.
- The ε_s and k_s/k_f are key factors for K_{yy}/k_f since they dominate the conduction heat transfer. However, the results do not agree with the mixing theory, $K^*_{yy} = \varepsilon_f k^*_f + \varepsilon_s k^*_s$, because of the geometry, and arrangement can lead to complex heat conduction patterns. If one does use the mixing theory one should realize their limitations.

8. Conclusion

We used the unit cell and volume averaging theorem based on microscope energy balance concept to develop the direct temperature solution method to solve for the modified effective thermal conductivity tensor as influenced by the unit cell structure, Peclet number of the fluid, volume fraction of the solid, thermal conductivity ratio of the solid and the fluid. This method simplifies the calculations by introducing a moving frame to convert the convective-diffusive energy equation to a pure conduction equation. The modified effective thermal conductivity tensor can help us to analyze the temperature history of a non-isothermal fluid flowing in a porous media. Especially for composite processing techniques such as resin transfer molding (RTM), the temperature is an important issue.

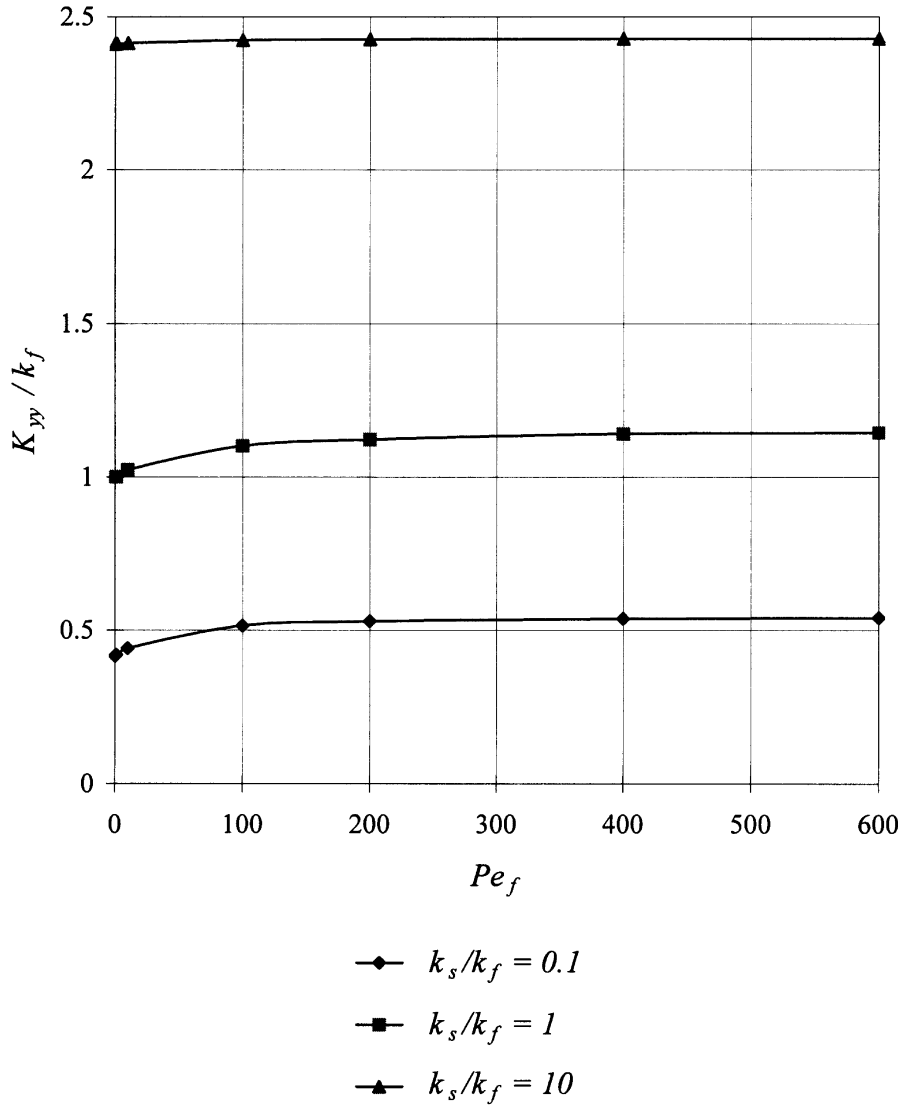

Fig. 11. The modified effective thermal conductivity perpendicular to the flow direction vs Peclet number (solid volume fraction of 50%).

The direct temperature solution method's main advantages are that one can physically relate temperature to the thermal conductivity concept and visualize the microscopic temperature field in a unit cell. The unit cell approach with $(\rho c_p)_s/(\rho c_p)_f = 1$ with proposed conditions is consistent with law of energy balance and has a unique solution. It is possible to handle more than one solid phase and fluid phase or even with a moving solid phase by this method. Based on the understanding of the physical quantity derived from simple mathematics, $\mathbf{u}_{pcf}$, $\langle \mathbf{q} \rangle$, and $\nabla \langle T \rangle$ we can explain and predict the trend of the modified effective thermal conductivity tensor more effectively.

Although the direct temperature solution allows for clear physical meaning and the visualization of microscopic temperature field inside the unit cell, it is still unable to predict the effect of $(\rho c_p)_s/(\rho c_p)_f$. This will be a topic of future study.

Acknowledgement

The support of the National Science Foundation Grant Number DDM-9203968 is gratefully acknowledged.

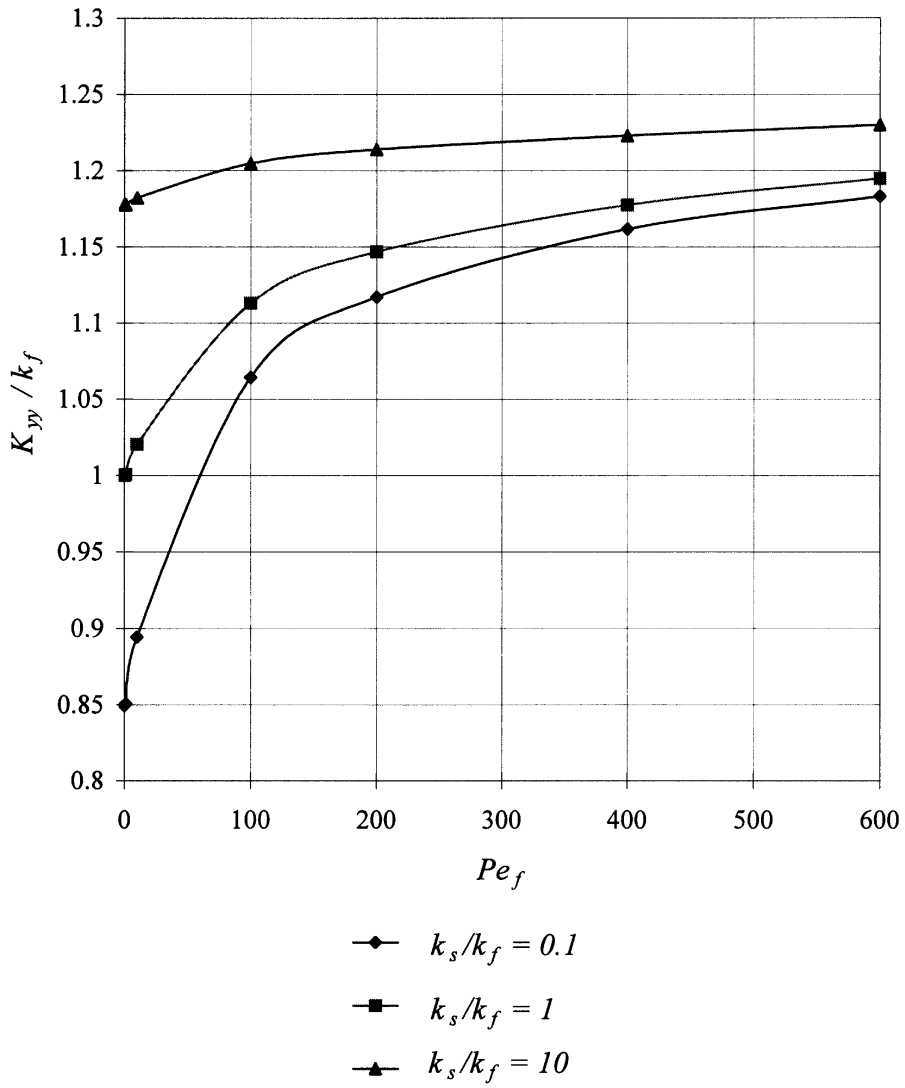

Fig. 12. The modified effective thermal conductivity perpendicular to the flow direction vs Peclet number (solid volume fraction of 10%).

References

[1] R.B. Dessenberger, C.L. Tucker, Thermal dispersion in resin transfer molding, Polymer Composites 16 (1995) 495–506.
[2] R.G. Carbonell, S. Whitaker, Dispersion in pulsed systems—II: theoretical developments for passive dispersion in porous media, Chem. Engng. Sci. 38 (1983) 1795–1802.
[3] Wei Zhang, S.G. Advani, Heat dispersion effects in stationary fiber beds, Mechanics in Materials Processing and Manufacturing ASME 194 (1994) 335–352.
[4] G.L. Tucker, R.B. Dessenberger, Governing equations for flow and heat transfer in stationary fiber beds, in: S.G. Advani (Ed.), Flow and Rheology in Polymer Composites Manufacturing, Elsevier Science, 1994, pp. 257–322.
[5] M. Sahraoui, M. Kaviany, Slip and no-slip temperature boundary conditions at interface of porous, plain media: convection, Int. J. Heat and Mass Transfer 37 (1994) 1029–1044.
[6] G.I. Taylor, Dispersion of soluble matter in solvent flowing slowly through a tube, Proc. R. Soc. Lond. A219 (1953) 186–203.
[7] D.J. Gunn, C. Pryce, Dispersion in packed beds, Trans. Inst. Chem. Engrs. 47 (1969) T341–T350.
[8] M. Kaviany, Principles of Heat Transfer in Porous Media, 2nd edn., Springer, New York, 1995, pp. 157–258.
[9] R. Aris, On the dispersion of a solute flowing slowly through a tube, Proc. R. Soc. Lond. A235 (1956) 67–77.
[10] A.E. Scheidegger, Statistical hydrodynamics in porous media, J. Appl. Phys. 25 (1954) 994–1001.

[11] G. De Josselin De Jong, Longitudinal and transverse diffusion in granular deposits, Trans. Amer. Geophys. Union 39 (1958) 67–74.
[12] P.G. Saffman, Dispersion due to molecular diffusion and macroscopic mixing in flow through a network of capillaries, J. Fluid Mech. 7 (1960) 194–208.
[13] F.J.M. Horn, Calculation of dispersion coefficient by means of moments, AIChE J. 17 (1971) 613–620.
[14] H. Brenner, Dispersion resulting from flow through spatially periodic porous media, Phil. Trans. Roy. Soc. (London) 297 (1980) 81–131.
[15] A. Eidsath, R.G. Carbonell, S. Whitaker, L.R. Herman, Dispersion in pulsed systems—III: comparison between theory and experiments for packed beds, Chem. Engng. Sci. 38 (1983) 1803–1816.
[16] D.L. Koch, R.G. Cox, H. Brenner, J.F. Brady, The effect of order on dispersion in porous media, J. Fluid Mech. 200 (1989) 173–188.
[17] C.C. Mei, Heat dispersion in periodic porous media by homogenization method, Multi. Trans. in Porous Media ASME. FED122/HTD 186 (1991) 11–16.
[18] Z. Yuan, W. Somerton, K.S. Udell, Thermal dispersion in thick walled tubes as a model of porous media, Int. J. Heat and Mass Transfer 34 (1991) 2715–2726.